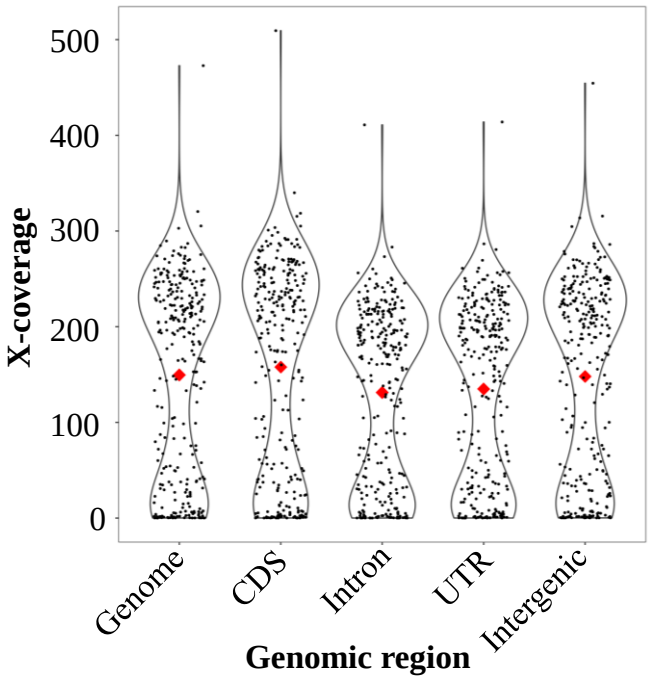

Supplementary Figure 1: X-coverage profile of genomes sequenced. Samples with at least 10X coverage were considered for downstream analysis.

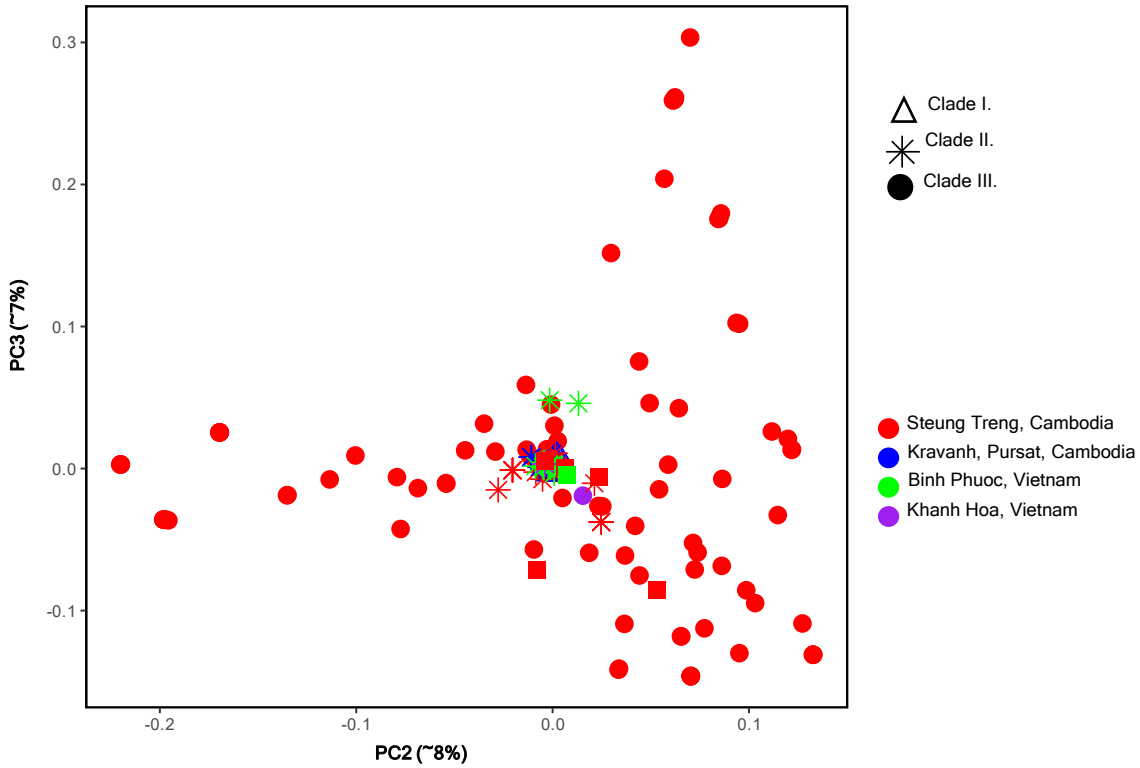

Supplementary Figure 2: PCA analysis. Principal components 2 and 3 describe the variability within East Cambodian samples. The pattern of clustering supports the distinguished clades from phylogenetic analysis.

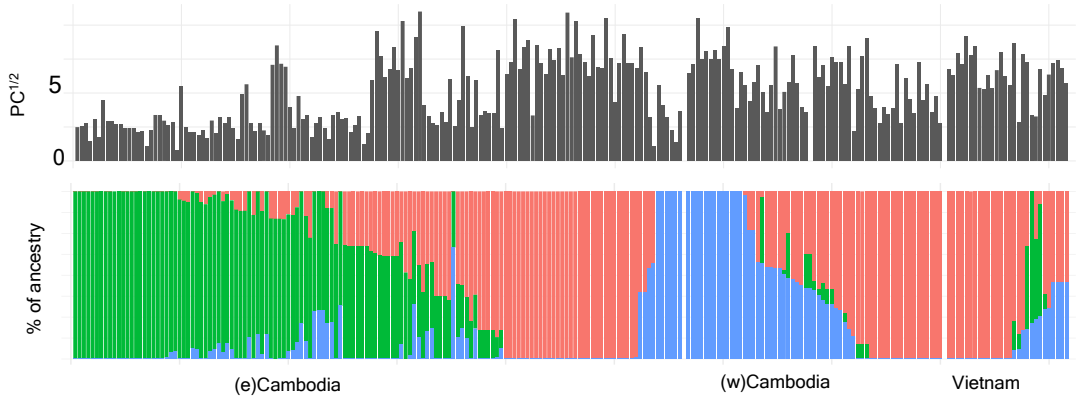

Supplementary Figure 3: Admixture population analysis of parasite population. The bar graph (at the bottom) shows the mixture of ancestries within parasites collected from three collection sites. The bar graph (on the top) shows the estimated parasite clearance half-life of each individual isolate. Strikingly a group of parasites from east Cambodia (left side of the plots) with more ancestral components marked by green bar was found mostly to have $PC^{1/2}$ < 5 hours (susceptible parasites).

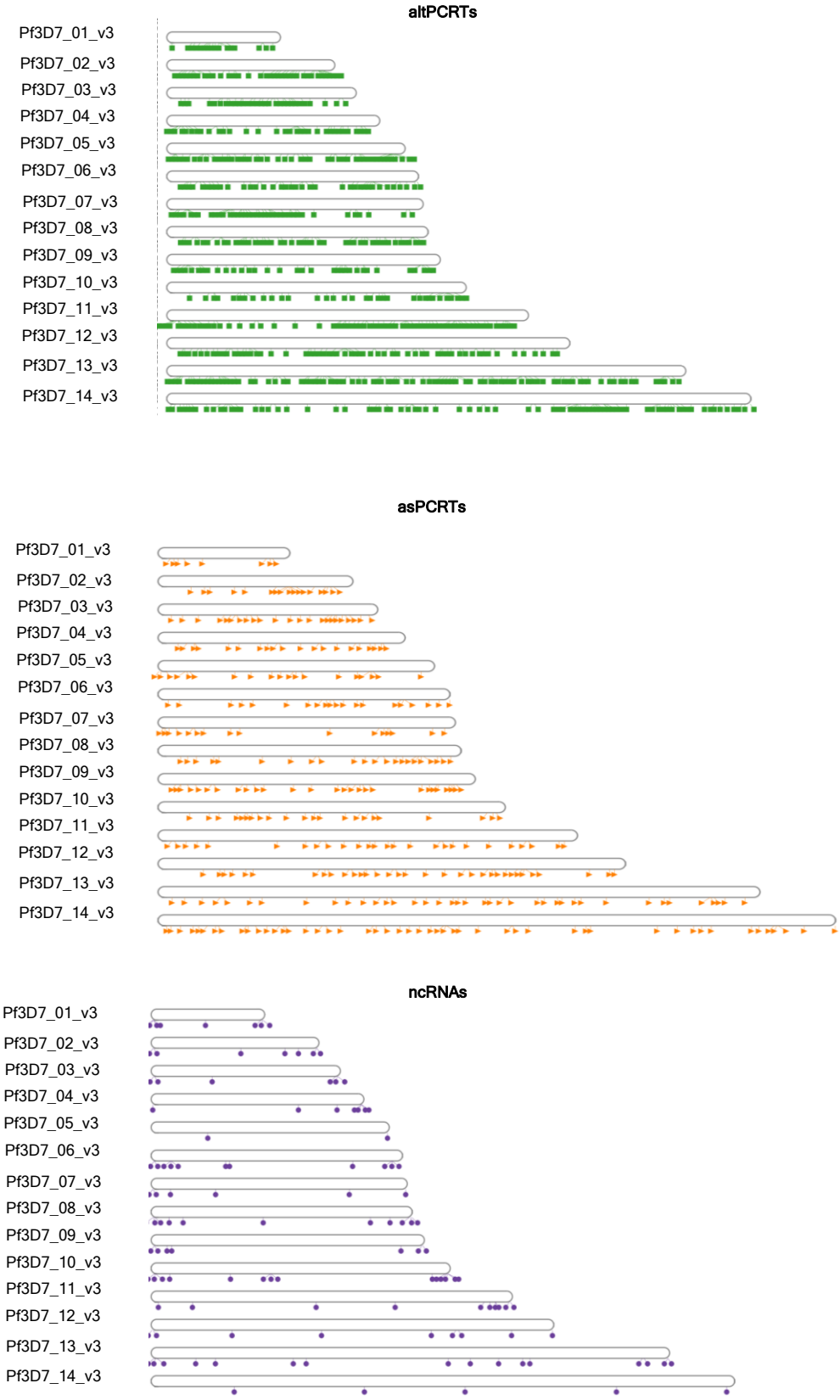

Supplementary Figure 4: Non-PCRTs' position across the chromosomes. A significant bias was observed for the localization of detected noncoding RNAs (ncRNAs) compared to detected alternatively spliced PCRTs (altPCRTs) and anti-sense PCRTs (asPCRTs). Most of the ncRNAs detected were found to be in the sub-telomeric repeat region.

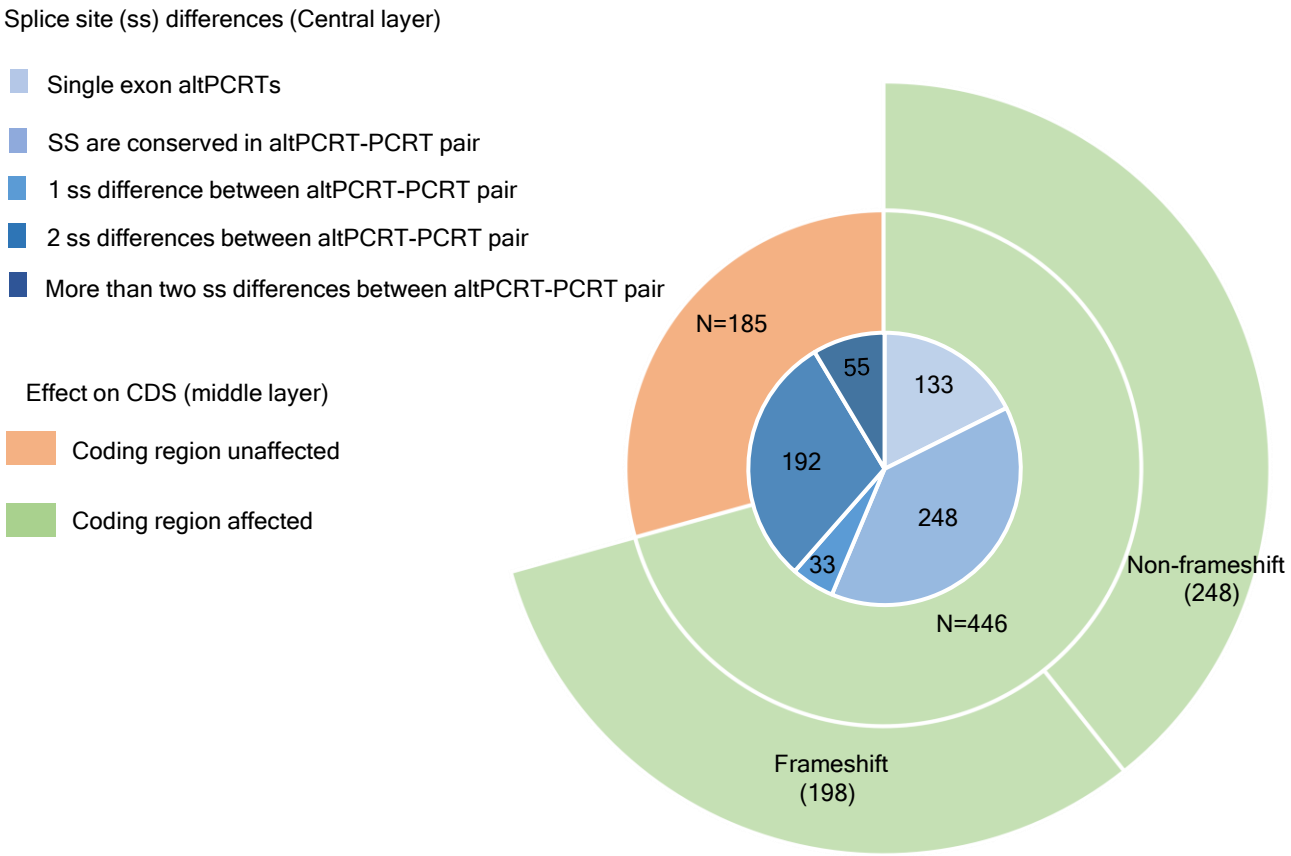

Supplementary Figure 5: Classification of detected alternatively spliced PCRTs. Comparing detected alternatively spliced PCRTs (Protein Coding Reference Transcripts) with overlapping PCRTs. (Central layer) First PCRT-altPCRT pairs were compared by differences in splice sites. (Middle layer) The second classification was based on coding region differences between the PCRT-altPCRT pair. (Outer layer) altPCRTs with coding region differences further investigated whether to have a frameshift or non-frameshift effect. Data from the central layer are independent of the middle and outer layers.

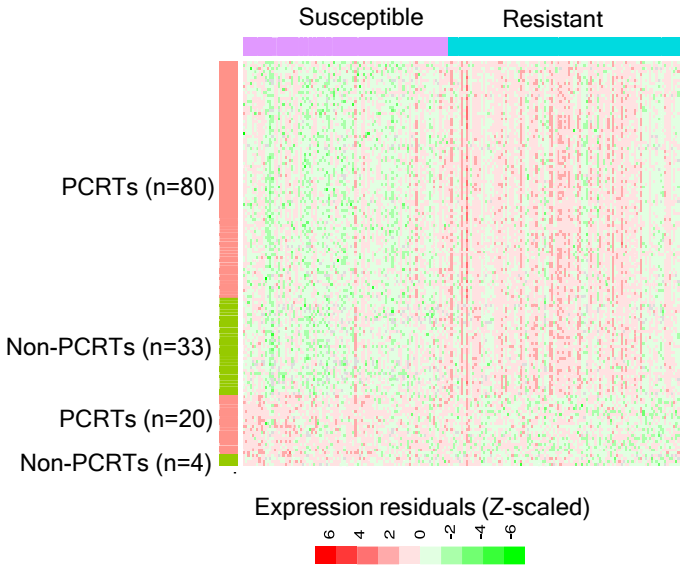

Supplementary Figure 6: Differentially expressed transcripts from hr0 transcriptomes. Heatmap of differentially expressed transcripts between susceptible and resistant parasites with FDR <0.05 totaling 100 PCRTs and 37 non-PCRTs.

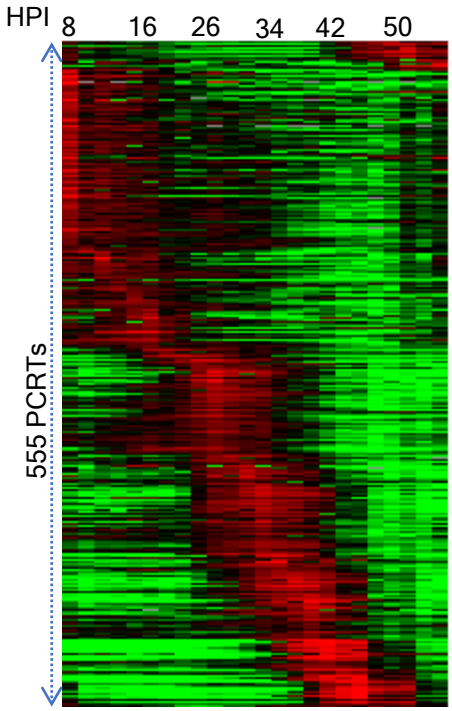

Supplementary Figure 7: In-vivo repressed PCRTs from IDC. Expression profiles of the PCRTs from intra-erythrocytic development cycle (IDC) repressed in resistant parasites upon 6 hours of exposure to ACT/TACT.

Supplementary Figure 8

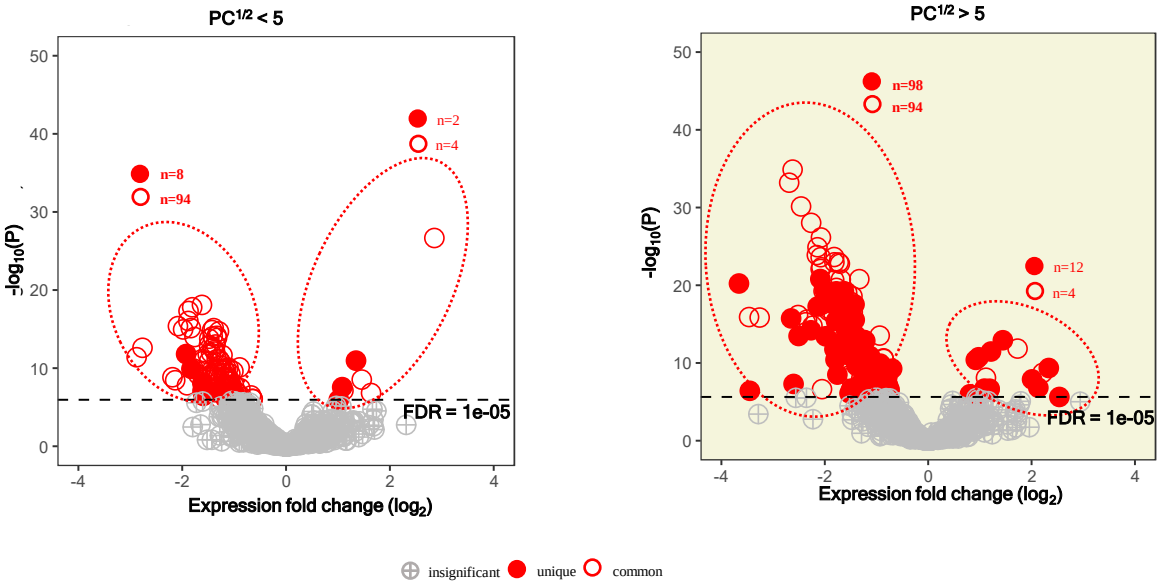

Supplementary Figure 8: In-vivo transcriptome response to drug through non-PCRTs. Induction or repression of non-PCRTs upon treatment with artemisinin combination therapy in susceptible (left) and resistant (right) parasite groups. Any transcripts with FDR < 1e-05 considered as significant and commonly induced/repressed transcripts are marked as un-filled red colored circles. The background and point color of the volcano plots is to differentiate the resistant parasites from susceptible parasites and PCRTs from non-PCRTs respectively. White and beige background signifies the parasite groups as Susceptible and resistant respectively, whereas red circles here represent significantly up-down-regulated non-PCRTs.

(a)

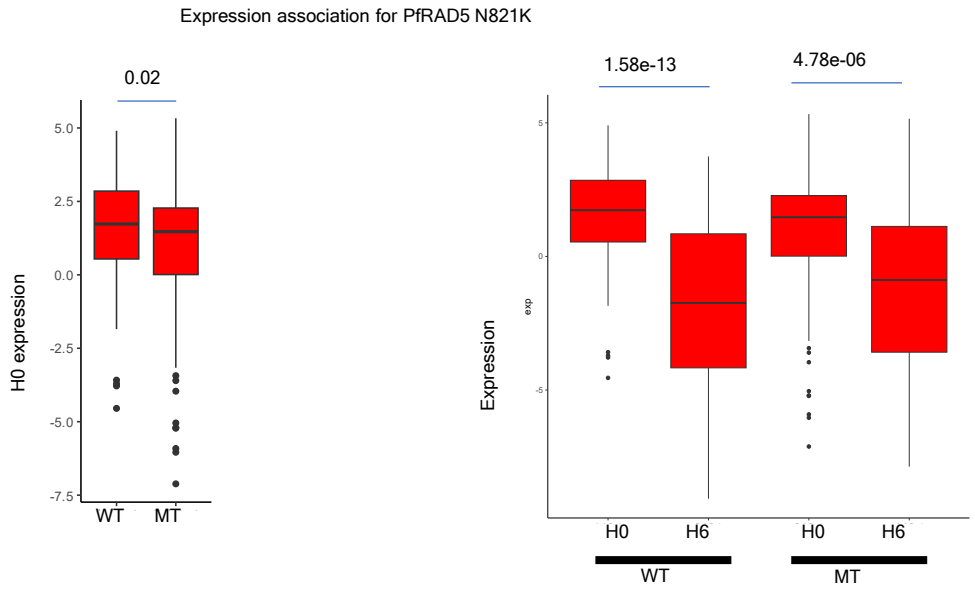

(b)

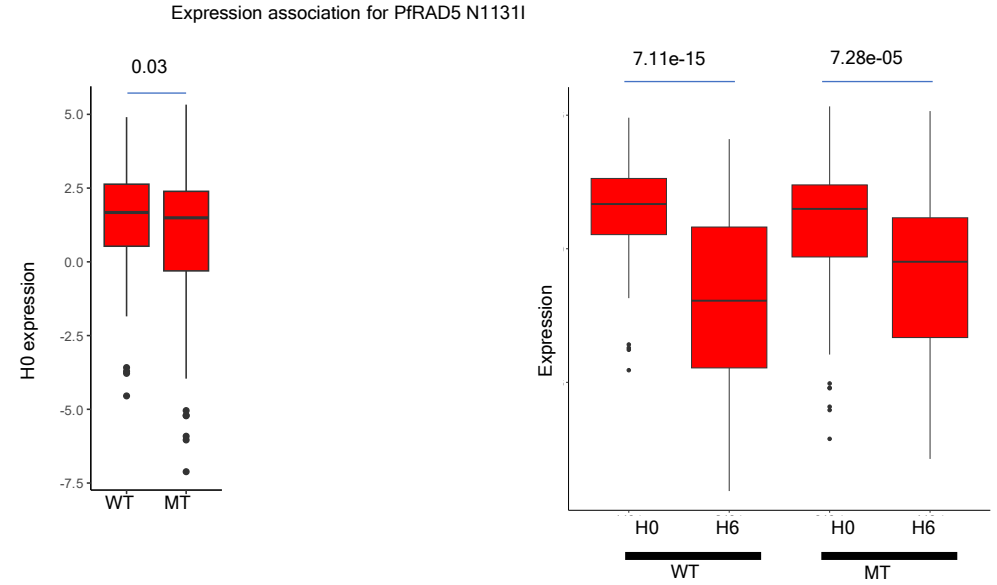

Supplementary Figure 9: Association between PfRAD5 mutations and altPfRAD5 expression. GWAS analysis detected two PfRAD5 mutations (N821K and N1131I) associated with parasite clearance half-life ($PC^{1/2}$). (a) An eQTL-like association was found for PfRAD5 N821K with expression of alternatively spliced PfRAD5 transcripts (left panel). Moreover, the expression of altPfRAD5 was repressed upon drug exposure in both resistant and susceptible parasites with a lower level of statistical significance for resistance parasites (right panel). (b) The second mutation, PfRAD5 N1131I, was found to be associated in an exactly similar way as PfRAD5 N821L.

(a)

Target	Forward primer	Reverse primer
Both isoforms	TGACCTTATGAACATTGATGAAAG	TCCATGGTACTTTTAATTTCTTGTG
Alternative isoform (altPCRT)	ATTTATTGGTTACTGCTTCTTGT	CCATGTTTATATTTTATTTAATTTTTTTCCCAACC
Canonical isoform (PCRT)	TATAATTGTTCAAAAGCATCACAAGAAA	TGGAATAGTGCACACCAAAAGA
PF3D7_0422300	GCAGTAGGTGGAGGTACAGG	GAGGAGATGGCCACGAACAA

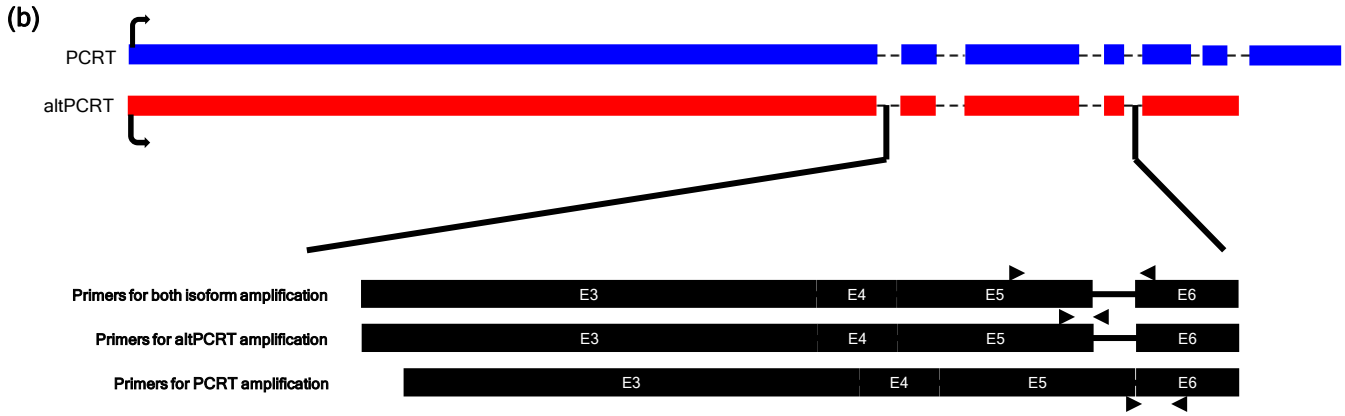

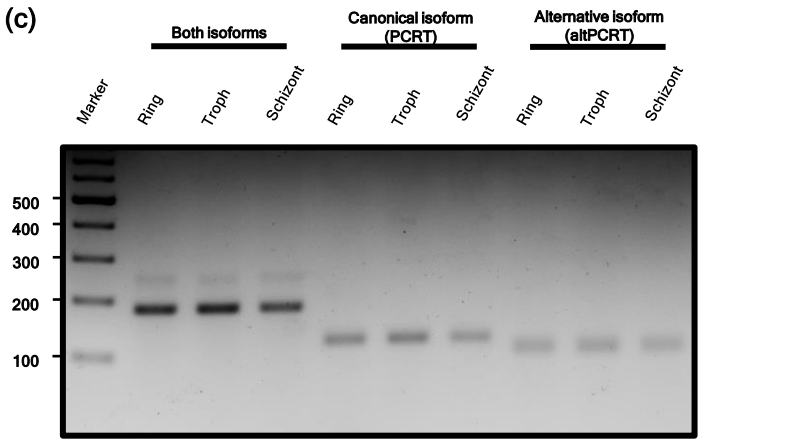

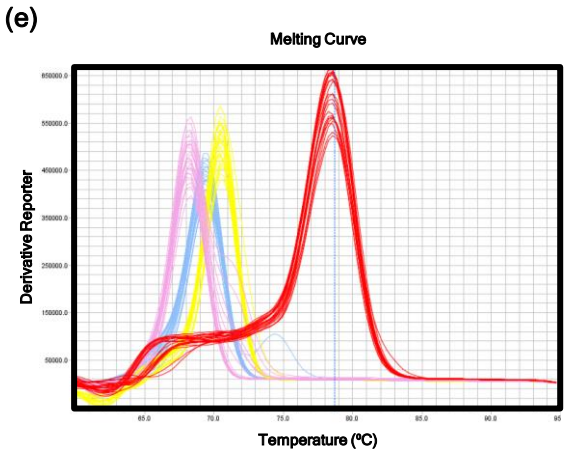

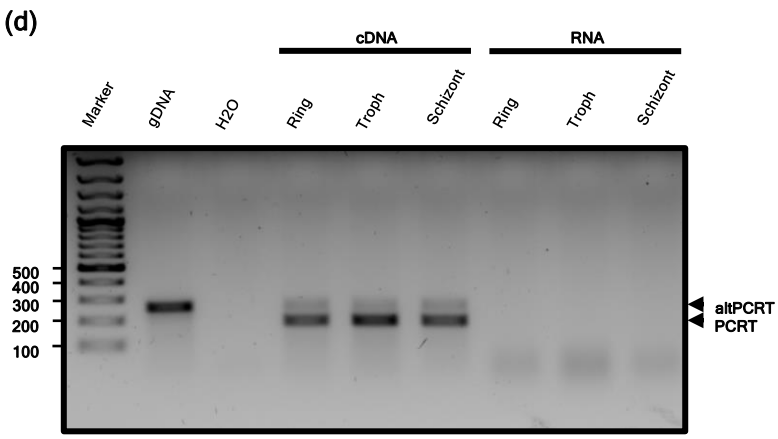

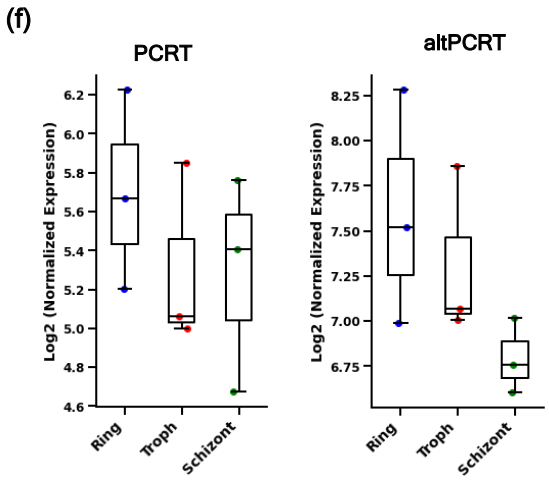

Supplementary Figure 10: RT-PCR Confirmation of Canonical and Alternative Isoforms of *PF3D7_1138800.* (a) Primer sequences for amplification of both isoforms, each individual isoform as well as the reference gene (*PF3D7_0422300*) in conventional PCR and quantitative PCR. (b) Gene architecture of canonical isoform (*PF3D7_1138800.1*) and alternative isoform (*MSTRG.5058.9)*, along with amplified domains in respective isoforms for PCR. (c) Amplification by all pairs of primers was successful as shown by the isoform-specific PCR products at expected size for all the sample in the electrophoresis gel. (d) The absence of gDNA contamination was verified by incorporating reverse transcription-free samples. Negative controls comprised water, whereas genomic DNA (gDNA) served as the positive control. (e) Confirmation of isoform specificity of the products via quantitative PCR melting curve analysis. (f) Isoform expression at different developmental stages of Plasmodium, as determined by qPCR employing the ddCt analysis method.

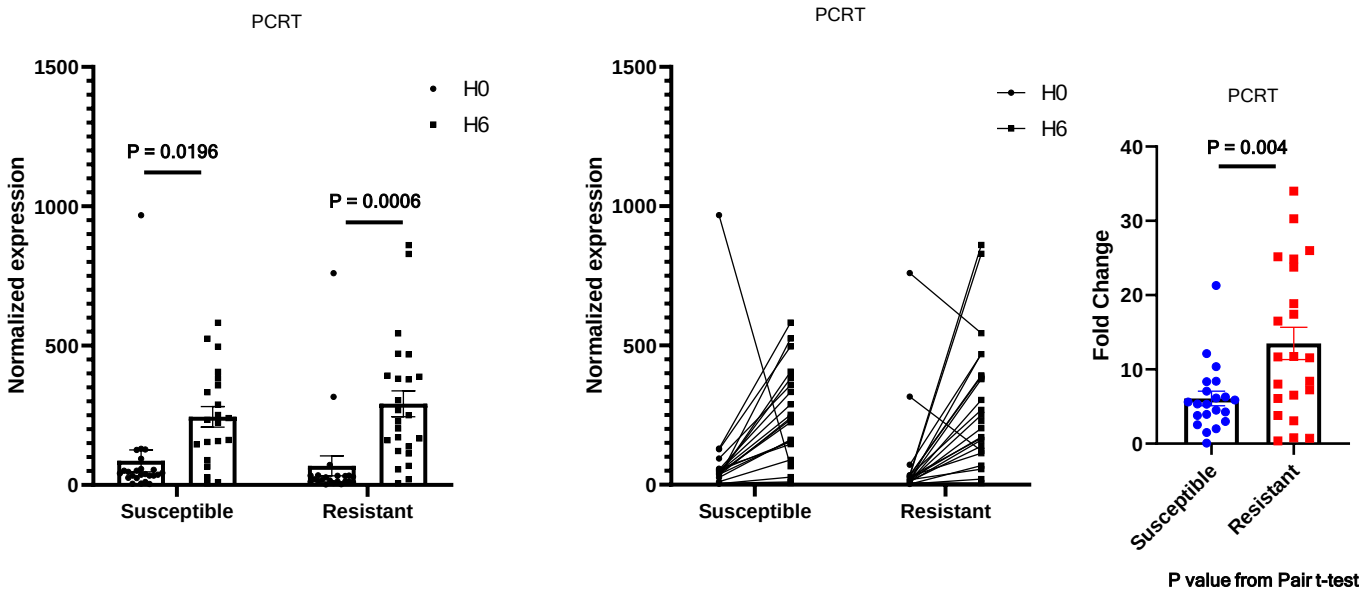

Supplementary Figure 11: Expression profile of the PfWD11 from qPCR experiment. Expression changes of the susceptible parasites and resistant parasites from 0 hours to 6 hours as groups (left) and as a pair (middle) respectively. Foldchange comparison between susceptible and resistant groups by Pairwise t-test. Point to be noted: that all qPCR validations on field isolates are solely performed with the purpose of detecting their presence not for expression correlation, as expression correlation depends on multiple factors parasite's age, the expression profile of the housekeeping genes, etc.

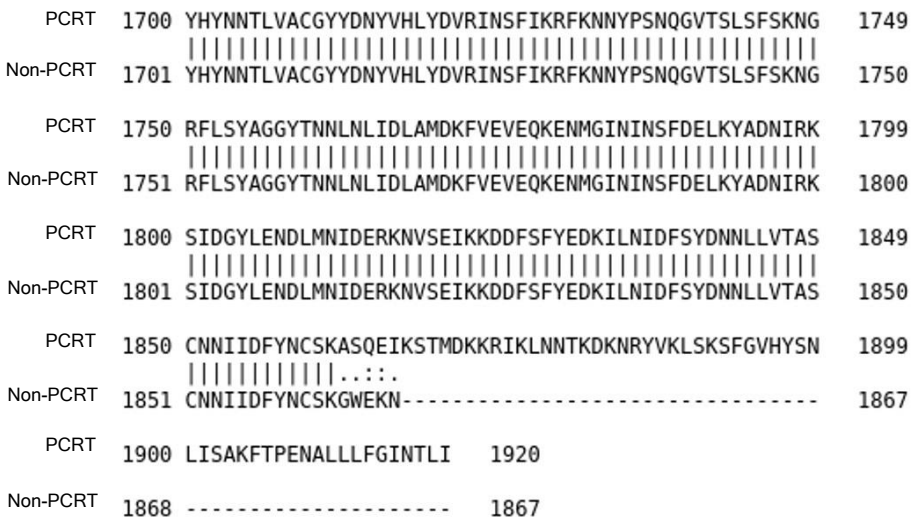

Supplementary Figure 12: Pair-wise sequence alignment of PCRT-altPCRT pair for PfWD11 protein. Retention of intron 5 in altPCRT leads to early truncation of the predicted open reading frame and indicates 58 missing amino acid residues compared to PfWD11 PCRT at the C-terminal.

(a)

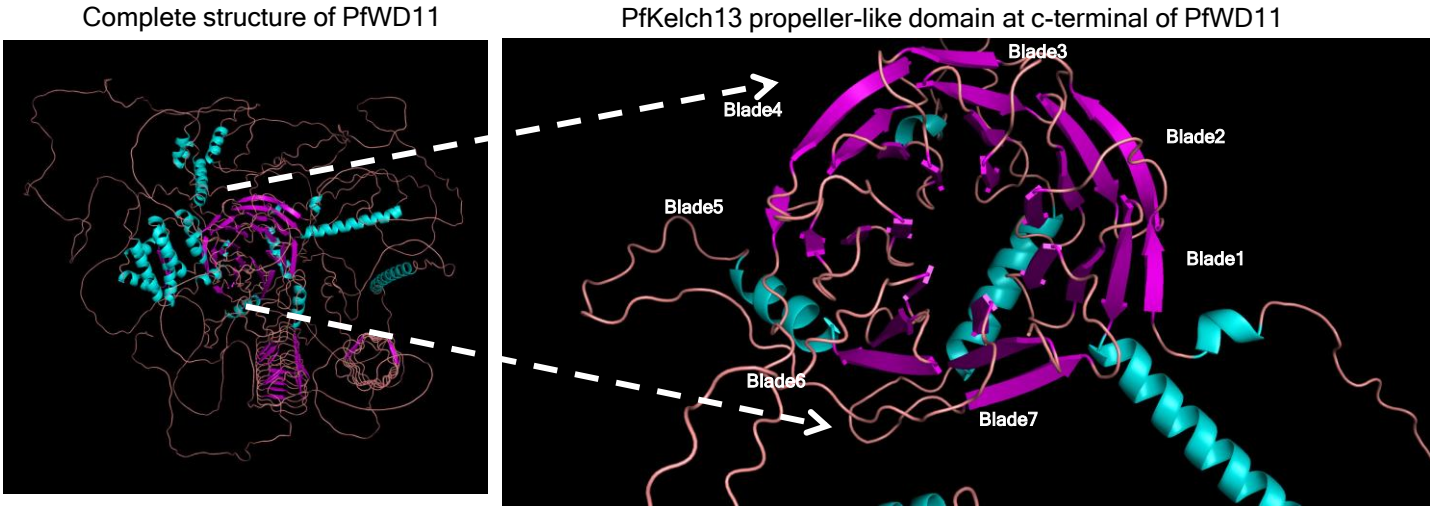

(b)

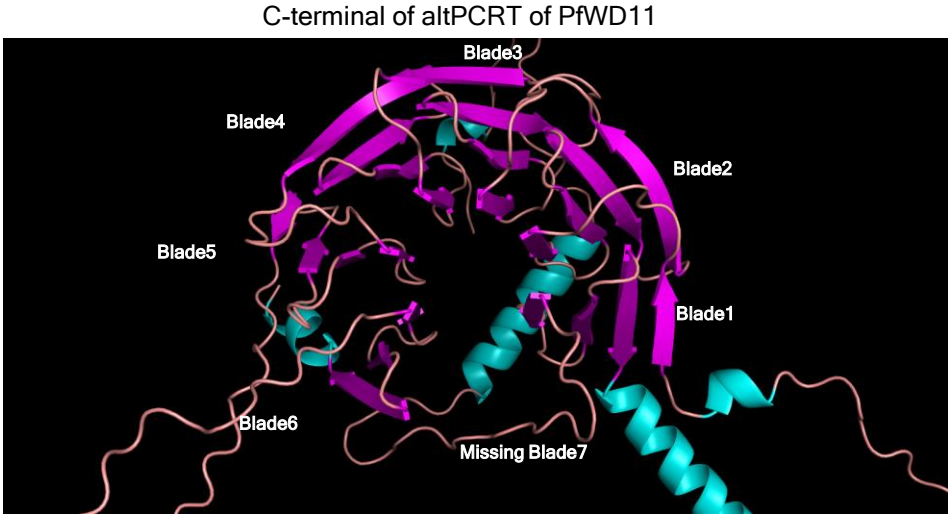

Supplementary Figure 13: Alpha fold predicted structure of PfWD11 (PCRT and altPCRT). (a) Alpha fold predicted structure of PfWD11 was obtained from the Uniprot database and visualized in PyMol. Noticeably the c-terminal of the PfWD11 was found to have a propeller-like domain similar to PfKelch13 (whose propeller domain mutations are known resistance markers for Artemisinin treatment). (b) The result of intron 5 retention leads to early truncation and missing blade 7, an integral part of the propeller domain, from the c-terminal structure of altPfWD11 predicted by alphafold.